# AutoATES AUSTRIA - TESTING AND APPLICATION OF AN AUTOMATED MODEL-CHAIN FOR AVALANCHE TERRAIN CLASSIFICATION IN THE AUSTRIAN ALPS

Andreas Huber[1,*], Christoph Hesselbach[1], Felix Oesterle[1], Michael Neuhauser[1], Marc Adams[1], Matthias Plörer[1], Laura Stephan[2], Havard B. Toft[3,4], John Sykes[5,6], Christoph Mitterer[2], Jan-Thomas Fischer[1]

[1]*Austrian Research Centre for Forests (BFW), Department of Natural Hazards, Innsbruck, Tyrol, Austria*
[2]*Avalanche Warning Service Tyrol, Innsbruck, Tyrol, Austria*
[3]*Norwegian Water Resources and Energy Directorate (NVE), Oslo, Norway*
[4]*Center for Avalanche Research and Education, UiT the Arctic University of Norway, Tromsø, Norway*
[5]*Geography Department, Simon Fraser University, Burnaby, British Columbia, Canada*
[6]*Chugach National Forest Avalanche Center, Girdwood, Alaska, USA*

ABSTRACT: The Avalanche Terrain Exposure Scale (ATES) has been widely adopted in Canada and also applied in different European mountain regions. Initial implementations relied on manual work-flows. However, advances in open-source data and software availability have sparked the development of automated work-flows and their application to areas in Norway, Canada, Switzerland, the Pyrenees, or Bulgaria. We apply an AutoATES work-flow for a $700\,\mathrm{km}^2$ model region in Tyrol, Austria. The work-flow comprises sub-modules for (i) potential release area (PRA) delineation, (ii) avalanche runout modeling, and (iii) a final classification step. Focus is laid on avalanches up to size 3 to capture avalanche situations and sizes typical for skier involvement. We informed parametrization of the sub-models by utilizing observational data from our study area and openly available data from other Alpine regions and evaluated results of the runout model for 100 randomly selected avalanches against expected dimensions of size 3 avalanches. Results indicate the applicability of the method for our region, but also highlight current limitations. The need for local adaptation of model parameters is emphasized and the use of a fourth "extreme terrain" class for areas like our pilot region is encouraged. Future developments should be directed towards introducing an additional PRA segmentation step, and an update of the avalanche runout model to better account for avalanche release area and track characteristics, and avalanche-forest interactions. An evaluation of automatically generated against manual ATES maps and a comparison of different classified avalanche terrain map products are still ongoing and expected to provide further insights.

*Keywords:* ATES, automated avalanche terrain classification, PRA modeling, avalanche runout modeling

## 1. INTRODUCTION

Besides meteorological conditions and snow-pack properties, terrain factors play an important role in avalanche formation (Schweizer et al., 2003). Consequently, adapting terrain choices in accordance with prevailing snow and meteorological conditions can be considered a key measure for managing risks in potential avalanche terrain (Landrø et al., 2020). Historically, professional and recreational backcountry-users have relied on manual terrain interpretation from topographic maps and observations in the field. The increasing availability of high resolution digital terrain models as well as the proliferation of mobile electronic devices and software applications has led to a shift from the use of mainly analog to increasingly digital cartographic products. Color-coded digital slope inclination maps have become a staple-item for trip planing in the winter back-country, and also more elaborate avalanche terrain map products have been suggested and published in recent years (e.g. Statham et al., 2006; Schmudlach and Köhler, 2016; Harvey et al., 2018; Larsen et al., 2020; Schumacher et al., 2022).

While avalanche terrain exposure scale (ATES) maps based on manual and semi-automated work-flows have been produced for areas in North America since the late 2000s (e.g. Statham et al., 2006; Delparte, 2008; Campell and Marshall, 2010; Campell and Gould, 2014), in the last 5 to 10 years also fully automated procedures for avalanche terrain maps have been developed. Amongst others Larsen et al. (2020) produced nation-wide ATES maps for Norway, Harvey et al. (2018) produced Categorized Avalanche Terrain (CAT) and Avalanche Terrain Hazard Maps (ATHM) for Switzerland and Schmudlach and Köhler (2016) also presented a method for production of automated avalanche terrain maps, which has been applied to

*Corresponding author address:
Andreas Huber, Austrian Research Centre for Forests (BFW), Innsbruck, Tyrol, Austria;
email: andreas.huber@bfw.gv.at

different mountain regions in Europe since. However, case-studies in the Austrian Alps have been scarce so far, with the exception of the maps based on Schmudlach and Köhler (2016), which have recently been made available on `skitourenguru.ch` and also cover the Austrian Alps.

The aim of our study was to test and apply an automated avalanche terrain mapping work-flow solely utilizing open-source software and data for a study area in the Austrian Alps. While the approaches of Schmudlach and Köhler (2016) and Harvey et al. (2018) have already yielded promising results in similar settings in the Swiss Alps and different European mountain regions, the methods partly rely on proprietary software. For this reason we decided to adapt and apply the AutoATES work-flow originally proposed by Larsen et al. (2020) and recently updated by Toft et al. (2023c) for which all model components have been published under an open-source license.

Similar to the Swiss ATHM and CAT maps (Harvey et al., 2018), we focused on adapting the AutoATES work-flow for medium to large avalanches ($\leq$ size 3 according to EAWS[1]) which are also most commonly expected for avalanche danger levels $\leq 3$ according to the EAWS danger scale[2]. Most professional and recreational users will frequent the potential avalanche terrain in our study area in these conditions.

## 2. METHODOLOGY

The AutoATES work-flow builds on recently developed open-source tools by different research groups and comprises three steps. These steps involve (i) the automated identification of potential avalanche release areas (PRAs), (ii) the delineation of potential run-outs of size $1$ to $3$ avalanches, and (iii) a final classification and mapping step. Within the last step information on modeled PRAs and avalanche run-outs is combined and interpreted with additional map-layers (slope incline, degree of forest cover, glacier extents) into discrete ATES classes (*simple*, *challenging*, *complex*, and *extreme*).

### *2.1. Study area and data*

We selected a $700\,\mathrm{km}^2$ model region located in the Austrian Alps, South-West of Innsbruck to test the AutoATES approach. The region covers parts of the Ötztal and Stubai Alps and is a popular destination for ski-touring in winter, with many easy to access trail-heads in avalanche terrain of varying complexity. Large portions of the study areas are characterized by high alpine terrain with elevations reaching up to almost $3500\,\mathrm{m}$, and about $5\%$ are still glacier covered. Figure 1 shows the location of the study area.

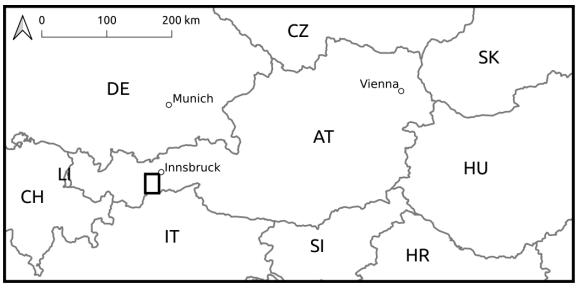


Figure 1: Location of the study area in the Austrian Alps. The rectangular outline encompasses the study area, which covers an area of $\approx 700\,\mathrm{km}^2$ in the Northern Stubai and North-Eastern Ötztal Alps.

#### 2.1.1. Digital Elevation Model

$1\,\mathrm{m}$ airborne lidar survey (ALS) based digital surface (DSM) and elevation models (DEM) are available for our study area and issued under a creative commons license (`data.tirol.gv.at`). While open-source high resolution DEMs ($1\,\mathrm{m} \times 1\,\mathrm{m}$, acquisition dates 2017 and 2018) were available for our study area, we decided to use a spatial resolution of $10\,\mathrm{m} \times 10\,\mathrm{m}$ for our case study. The coarser resolution significantly reduces required computational times an is in line with raster resolutions reported by Larsen et al. (2020) and Schumacher et al. (2022). The $10\,\mathrm{m}$ DEM has been derived from mosaicked $1\,\mathrm{m}$ DEM-tiles by bilinear resampling.

#### 2.1.2. Forest Layer

Different studies suggest, that including forest parameters in different stages of the model-chain improves the final map product. While Harvey et al. (2018) and Bühler et al. (2022) used binary forest-masks to exclude potential release areas in forested terrain and also take into account braking effects of forests on small to medium sized avalanches, Sharp (2018), Schumacher et al. (2022), or Sykes et al. (2022) also explore the use of different non-binary forest-maps in PRA delineation and avalanche terrain classification.

In our study we use a simplified approach to derive the degree of forest cover for each $10\,\mathrm{m} \times 10\,\mathrm{m}$ map pixel in our study area. We derive a $1\,\mathrm{m} \times 1\,\mathrm{m}$ normalized digital surface model (nDSM) by subtracting the DEM from the DSM. We then apply a $5\,\mathrm{m}$ threshold (Schumacher et al., 2022) on the nDSM, assigning a value of $1$ to values above and $0$ below this threshold. Subsequently this binary $1\,\mathrm{m}$

[1] `https://www.avalanches.org/standards/avalanche-size/`

[2] `https://www.avalanches.org/wp-content/uploads/2022/09/European_Avalanche_Danger_Scale-EAWS.pdf`

raster is aggregated to $10\,\mathrm{m}$ by simply summing up all $1\,\mathrm{m}$ cells inside the $10\,\mathrm{m}$ cells (e.g. Sykes et al., 2022), resulting in a raster with values ranging from $0$ (no forest cover) to $100$ (full forest cover). Eventually we apply a national binary forest layer[3] (Bauerhansl et al., 2007), also issued under a CC license, to mask out positive nDSM areas outside of forest areas (buildings, power-lines, bridges, etc.). The dataset is hereafter referred to as *percentage of forest cover* (PFC).

### 2.2. PRA delineation

A range of different algorithms for semi- and fully-automated delineation of PRAs has been developed in the past decades (e.g. Maggioni et al., 2002; Maggioni and Gruber, 2003; Rauter et al., 2006; Bühler et al., 2013; Veitinger et al., 2016; Bühler et al., 2018). In this study we utilize an adapted version of the fuzzy-logic-based PRA algorithm suggested by Veitinger et al. (2016), which was later modified by Sharp (2018) to include forest information and has also been used by Larsen et al. (2020) and Schumacher et al. (2022). While the original algorithm has been published in the R-language[4], we use a python version of the algorithm tailored to $10\,\mathrm{m}$ raster resolution[5].

Because of lacking data on documented release areas in our study site we utilized a dataset of documented avalanche release areas around Davos (Bühler and von Rickenbach, 2018; Bühler et al., 2018) to compare and test different variants of the PRA algorithm against observed PRAs and select a suitable threshold for converting fuzzy PRA membership values $\in \{0, \ldots, 1\}$ into binary release areas required for the runout-modeling. We found that an approach that utilizes a fuzzy combination of slope angle, windshelter-index (Winstral et al., 2002; Plattner et al., 2006) and PFC (see sec. 2.1.2) with terrain-ruggedness (Sappington et al., 2007) implemented as a binary mask performed well in comparison with the documented PRAs and also yielded satisfying results for our study area (Hesselbach, 2023).

### 2.3. Avalanche Runout estimation

While the initial AutoATES v1.0 work-flow (Larsen et al., 2020) used the *dinfAvalanche* function implemented in the hydrological toolbox TauDEM (Tarboton, 2016), Schumacher et al. (2022) and Toft et al. (2023c) recently used Flow-Py (D'Amboise et al., 2022) for modeling avalanche runouts from the delineated PRAs. Both runout models combine a simple travel-angle concept (Heim, 1932; Körner, 1980) for runout lenght estimation with hydrologically motivated flow algorithms for routing of flow paths in gridded elevation models (e.g. Horton et al., 2013; Wichmann, 2017).

We also utilized Flow-Py for runout modeling and tried to identify a suitable $\alpha$ angle for runout estimation of size 3 avalanches by comparison of model results with varying $\alpha$ against a limited set of 19 observed avalanches ($\approx$ size 3), which have been mapped from oblique aerial and terrestrial photographs. The remaining model parameters (exp, $z_\delta^{max}$, $R_{stop}$, cf. D'Amboise et al., 2022)) were chosen in accordance with D'Amboise et al. (2021). Table 1 lists all used Flow-Py model parameters.

In order to evaluate how well the runout model parameterisation is able to reproduce size 3 avalanches, we manually delineated single PRAs and selected a random subset of 100 PRAs in the size range of $10000 - 100000\,\mathrm{m}^2$ in our study area. Under the assumption of an average release thickness of $0.5\,\mathrm{m}$ (cf. Harvey et al., 2018) the release volumes of these PRAs fall into the range of $5000 - 50000\,\mathrm{m}^3$, thus being roughly representative of small to large size 3 avalanches (typical size 3 volumes of $\approx 10000\,\mathrm{m}^3$ after EAWS, entrainment is neglected in this assumption).

We then compared model results for these 100 avalanches in terms of projected travel length, affected area and peak pressure with expected value ranges for large avalanches (size 3) based on different suggested size classifications (see table 2). We modified the Flow-Py code to provide travel length outputs, and used an additional post-processing step to derive total affected areas, and the $99^{th}$ percentiles of travel lengths and impact pressures for each modeled avalanche. Impact pressures were calculated from modeled energy-line heights $z_\delta$ by estimating velocities with $v = (2\,g\,z_\delta)^{\frac{1}{2}}$ (cf. Körner, 1980) and assuming a density $\rho = 200\,\mathrm{kg\,m^{-3}}$ (Hesselbach, 2023).

Table 1: Utilized Flow-Py parameterisation for modeling of avalanches with size $\leq 3$ according to EAWS.

| parameters: | $\alpha$ | exp | $R_{stop}$ | $z_\delta^{max}$ |
|---|---|---|---|---|
| used values: | $26°$ | 8 | $3 \times 10^{-4}$ | $270\,\mathrm{m}$ |

### 2.4. Classification and Mapping

In the final classification or mapping step the information on the terrain inclination, modeled PRAs, outputs of the avalanche runout model, and additional layers (PFC, glaciers) are combined into discrete ATES classes. In principal we follow the

[3] https://inspire.lfrz.gv.at/000605/ds/BFW_Waldkarte.gpkg

[4] https://github.com/jocha81/Avalanche-release

[5] https://github.com/hvtola/potential_release_areas

Table 2: Avalanche size classification from different sources. tl = projected travel lenght based on EAWS, aa = affected area after Bühler et al. (2019), pp = peak pressure based on CAA (2016) (cf. Hesselbach, 2023).

| size | class | tl [m] | aa [$m^2$] | pp [kPa] |
|---|---|---|---|---|
| small | 1 | $\leq 50$ | $\leq 500$ | $\leq 5$ |
| medium | 2 | 50 – 200 | 500 – 10000 | 5 – 50 |
| large | 3 | 200 – 1000 | 10000 – 80000 | 50 – 250 |
| very large | 4 | 1000 – 2000 | 80000 – 150000 | 250 – 750 |
| extremely large | 5 | $\geq 2000$ | $\geq 150000$ | $\geq 750$ |

methodology outlined in Schumacher et al. (2022) with some modifications and parameter adaptions. We additionaly introduced a binary glacier layer (Austrian National Glacier Inventory 2015, Buckel and Otto (2018)) to disallow simple terrain on glaciers in accordance with Statham et al. (2006) and delineated a fourth *extreme terrain* class as suggested by Statham (2020) and Statham and Campell (2023) and similary implemented in the Swiss CAT and ATHM maps (Harvey et al., 2018). Figure 2 outlines the utilized classification work-flow, where the PRA and Flow-Py inputs correspond to the results of the PRA and avalanche runout-modeling steps discussed earlier. We also compared different parameter settings for the classification steps (Hesselbach, 2023).

Table 3: Input parameters for the classification step of the AutoATES work-flow based on analysis by Hesselbach (2023). SAT = slope angle threshold, AAT= $\alpha$ angle threshold, PFC = percent forest cover, ISL-SIZE = parameter used for cartographic generalization of the final map product (minimal required island size for 1 contiguous ATES area).

| parameter | value |
|---|---|
| SAT12 | $28°$ |
| SAT23 | $39°$ |
| SAT34 | $45°$ |
| AAT12 | $26°$ |
| AAT23 | $36°$ |
| PFC1 | 10 |
| PFC2 | 25 |
| PFC3 | 65 |
| ISL-SIZE | $1000\,m^2$ |

## 3. RESULTS & DISCUSSION

### *3.1. Runout modeling*

Figure 3 shows the results of the comparison of modeled against observed runout distances for varying $\alpha$ angles for the 19 mapped avalanches in our study area. Values of $\alpha$ between $26°$ and $28°$ show the best correspondence with observed avalanche travel lengths, while values $> 28°$ and $< 26°$ lead to under- and overestimation of runout lengths. This result is in accordance with the mean and standard deviation of observed travel-angles ($\bar{\alpha} = 26.8°$, $s_\alpha = 3.54°$). From the best-fitting $\alpha$ angles we used the more conservative $26°$ for our runout model (cf. tab. 1) and consequently also as the delimiter of *simple* and *challenging* avalanche terrain in the ATES classifier (AAT12, tab. 3).

Table 4: Percentage of Flow-Py model results with the used parameterisation (tab. 1) that fall above, within, and below the size 3 classification ranges for travel length (tl), affected area (aa) and peak pressure (pp) as defined in table 2.

| parameter: | tl | aa | pp |
|---|---|---|---|
| % above size 3 range: | 34% | 74% | 66% |
| **% within size 3 range:** | **57%** | **26%** | **33%** |
| % below size 3 range: | 4% | – | 1% |

Table 4 summarizes the results of the evaluation of the used Flow-Py parameterisation (table 1) for 100 randomly selected release areas against expected value ranges of size 3 avalanches (table 2). Modeled travel lenghts correspond with expected size 3 travel lenghts in $57\%$ of cases, while in $34\%$ of cases size 3 travel lengths are exceeded, and in $4\%$ not reached by the model. For affected areas and peak pressures about a quarter and a third of modeled avalanches fall within the expected range, while in almost all other cases expected size ranges are exceeded.

These results can partly be attributed to the inability of the simple runout model and used global value for $\alpha$ to be representative of size 3 avalanches. This is not surprising given the large intra-size-class spread of observed travel-angles $\alpha$ in our small observational dataset, which is also apparent in much larger datasets (Larsen, 2021), as well as the potentially weaker-than-expected correlation of $\alpha$ with avalanche size (cf. Toft et al., 2023a). Substituting the $\alpha$ angle model with an $\alpha - \beta$ type (e.g. Toft et al., 2023a) or physically-based model (e.g. Tonnel et al., 2023) might present an improvement, but would require previous segmentation of PRAs (cf. Bühler et al., 2018, 2022) or single contiguous avalanche paths.

Besides, the size-class correspondence is also influenced by the utilized size-classification scheme (e.g. EAWS, CAA, Bühler et al. (2019)) and employed classification criteria (travel length, pressure, affected area, ...) pointing to a general challenge in avalanche size classification (Hesselbach, 2023).

Nevertheless, our evaluation indicates, that modeled travel lengths are within size 3 range for almost $60\%$ of cases, while the remainder is overestimated, suggesting that the parameter choice for the runout modeling step is leaning towards the conservative side considering the scope of our application.

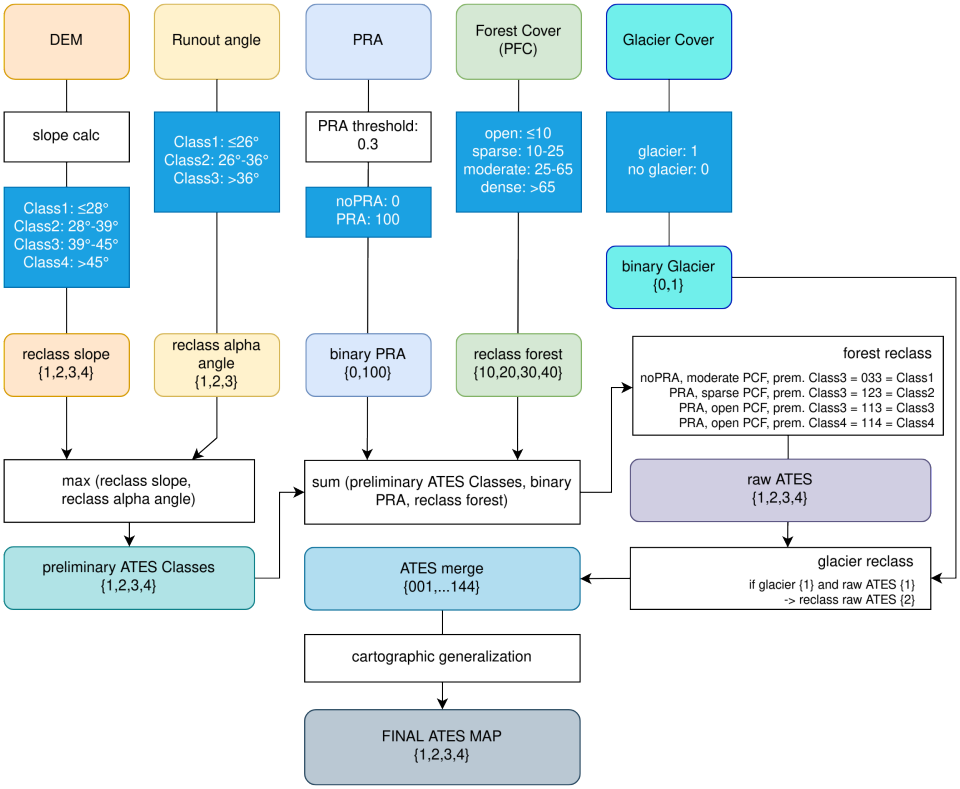


Figure 2: Flowchart highlighting the processing steps of the employed automated ATES algorithm. The parameters listed in table 3 (SAT, AAT, PCF) correspond to the class borders in the reclassification steps for the slope, runout-angle (Flow-Py output) and PFC layers.

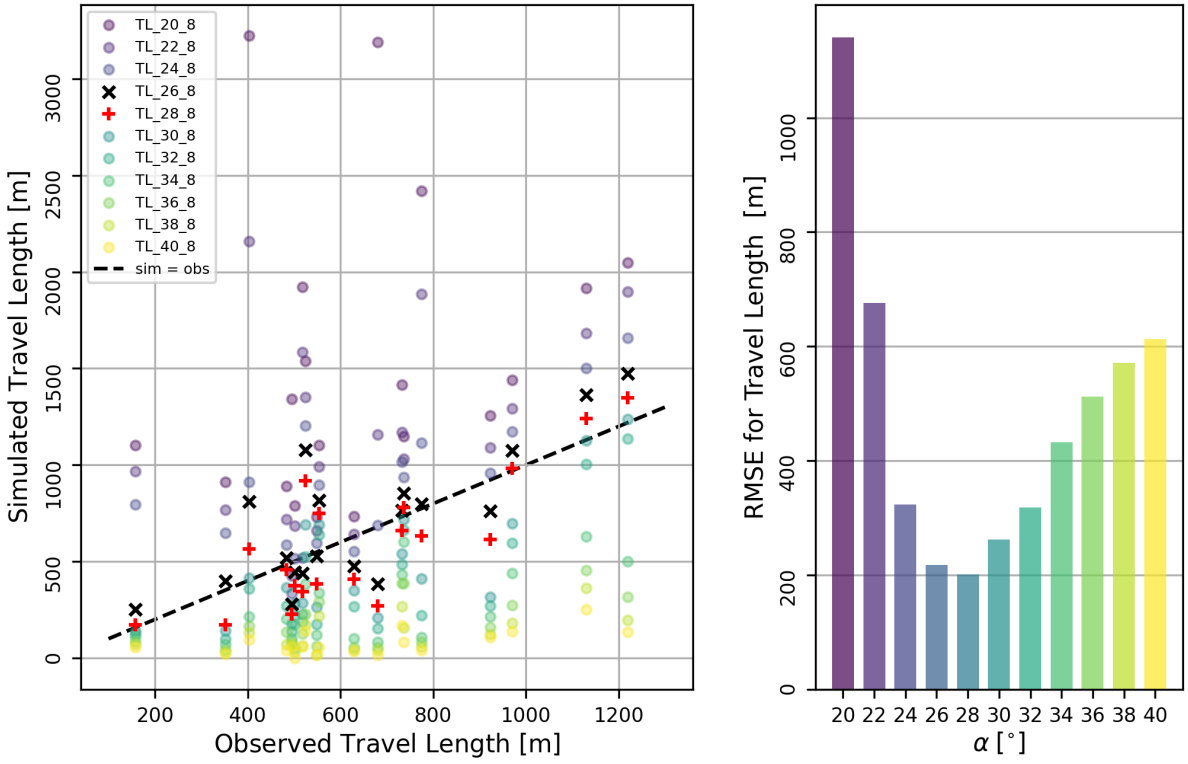


Figure 3: Comparison of modeled vs. observed runout lenghts for 19 ≈size 3 avalanches in the study area for different travel-angles $\alpha \in \{20°, 22°, \ldots, 38°, 40°\}$. The left figure shows a pair-wise comparison of observed and modeled travel lenghts [m] for the 19 avalanches; different colors indicate used $\alpha$ angles, the dashed black line corresponds to a 1:1 fit and results for $\alpha \in \{26°, 28°\}$ are overlaid by black x and red cross markers. The right figure shows the RMSE over all 19 avalanches for each $\alpha$. Best correspondence is found for $\alpha$ angles of 26° and 28°.

### 3.2. Classification and Mapping

Figure 4 shows the ATES map produced with the described parametrization (cf. tables 1 and 3) for two extracts of the study area. The lower panel in figure 4 highlights the influence of the utilized glacier layer, which results in otherwise flat, but glaciated terrain being classified into the *challenging* class. In both panels also the effect of the inclusion of a fourth *extreme* terrain class becomes apparent. Namely the *extreme* class allows distinguishing between terrain, where danger of falling might outweigh avalanche danger in the majority of cases. A similar differentiation has also been made in the Swiss CAT and ATHM map products (Harvey et al., 2018) and can be used to distinguish ski-able from generally non-ski-able terrain. We defined *extreme* terrain in this study as terrain with slope inclination $\theta \geq 45°$, however this threshold is subject to discussion and can be adjusted to local conditions and DEM resolution. In addition we also found, that inclusion of a forest layer in the PRA and classification step improved the overall map product, which is in alignment with previous studies (Schumacher et al., 2022; Sykes et al., 2022). However, forest information has not been used in the runout modeling step, which would be desirable in some cases (Hesselbach, 2023) and has shown promising results in AutoATES applications to different study sites (Toft et al., 2023c). It is also notable that the used parameters (table 1, 3) for our study area (esp. SAT and AAT) are significantly different from previous applications of AutoATES in Norway (Schumacher et al., 2022; Sykes et al., 2022) or Canada (Toft et al., 2023c). We deviate from the SAT thresholds for terrain incline as proposed in the ATES technical model (Statham et al., 2006; Statham and Campell, 2023) in this study to better reflect the technical difficulty encountered by back-country skiers when traveling over terrain of varying slope incline (thus, e.g. considering terrain below $28°$ to be generally *simple* to navigate). The higher values for AAT as compared to previous applications partially also address the problem, that more conservative values would lead to a large portion of *complex terrain* in typical Alpine settings as reported by Harvey et al. (2018) and also reflect the focus on avalanches of size $\leq 3$ in this study.

In general preliminary evaluation of the final map product indicates that the utilized parameterisation provides a balanced distribution of different terrain classes for our study area in reasonable agreement with expert-based assessment for selected areas and a validation dataset of observed avalanche runouts (Hesselbach, 2023). An evaluation against manually mapped ATES classes and a comparison of different avalanche terrain maps for the study area are currently still ongoing and, once finished, will also allow a more formal evaluation of the outlined method.

## 4. CONCLUSION & OUTLOOK

We successfully adapted and applied the open-source AutoATES work-flow, previously applied in Norwegian and North-American study sites to a $700\,\mathrm{km}^2$ study area in the Austrian Alps. We found that the introduction of a fourth *"extreme"* terrain class provides valuable additional information for our study area. Around $5\%$ of our study area is comprised of glaciated terrain. In accordance with the original ATES technical model (Statham et al., 2006), we used a national glacier inventory to assign glaciers at least to the challenging category. We argue that information on glacier extent is valuable for our test area, especially in early winter season. Whether or not to directly include glaciers in the ATES classes or not is subject to discussion. Compared to parameter settings used in different case-studies outside the Alps (e.g. Larsen et al., 2020; Schumacher et al., 2022) we found larger $\alpha$ angles (AAT) and slope angle thresholds (SAT) to be suitable for our study area.

The obtained results indicate, that the AutoATES work-flow can be applied also in typical Alpine settings. However, also some current limitations of the approach could be identified. Specifically the presented PRA delineation method is lacking functionality for automated segmentation of PRAs, which in turn would also be required for more sophisticated runout modeling approaches ($\alpha$–$\beta$, physically-based models, avalanche-forest interactions). While these limitations might be addressed in future studies, currently already a comparison of different available map-products for Austrian and Swiss study-sites (AutoATES, CAT) and the production of a manual ATES map for comparison with the AutoATES product are ongoing.

## ACKNOWLEDGEMENT

The presented work has been conducted with financial support of the AaATES project and the open Avalanche Framework AvaFrame (`https://www.avaframe.org`, last access: 15.08.2023). AaATES is a cooperation between the Federal Research Centre for Forests (BFW) and the Avalanche Warning Service Tyrol. AvaFrame is a cooperation between the Austrian Research Centre for Forests (Bundesforschungszentrum für Wald; BFW) and the Austrian Avalanche and Torrent Control Service (Wildbach- und Lawinenverbauung; WLV) in conjunction with the Austrian Federal Ministry of Agriculture, Forestry, Regions and Water Management (BML).

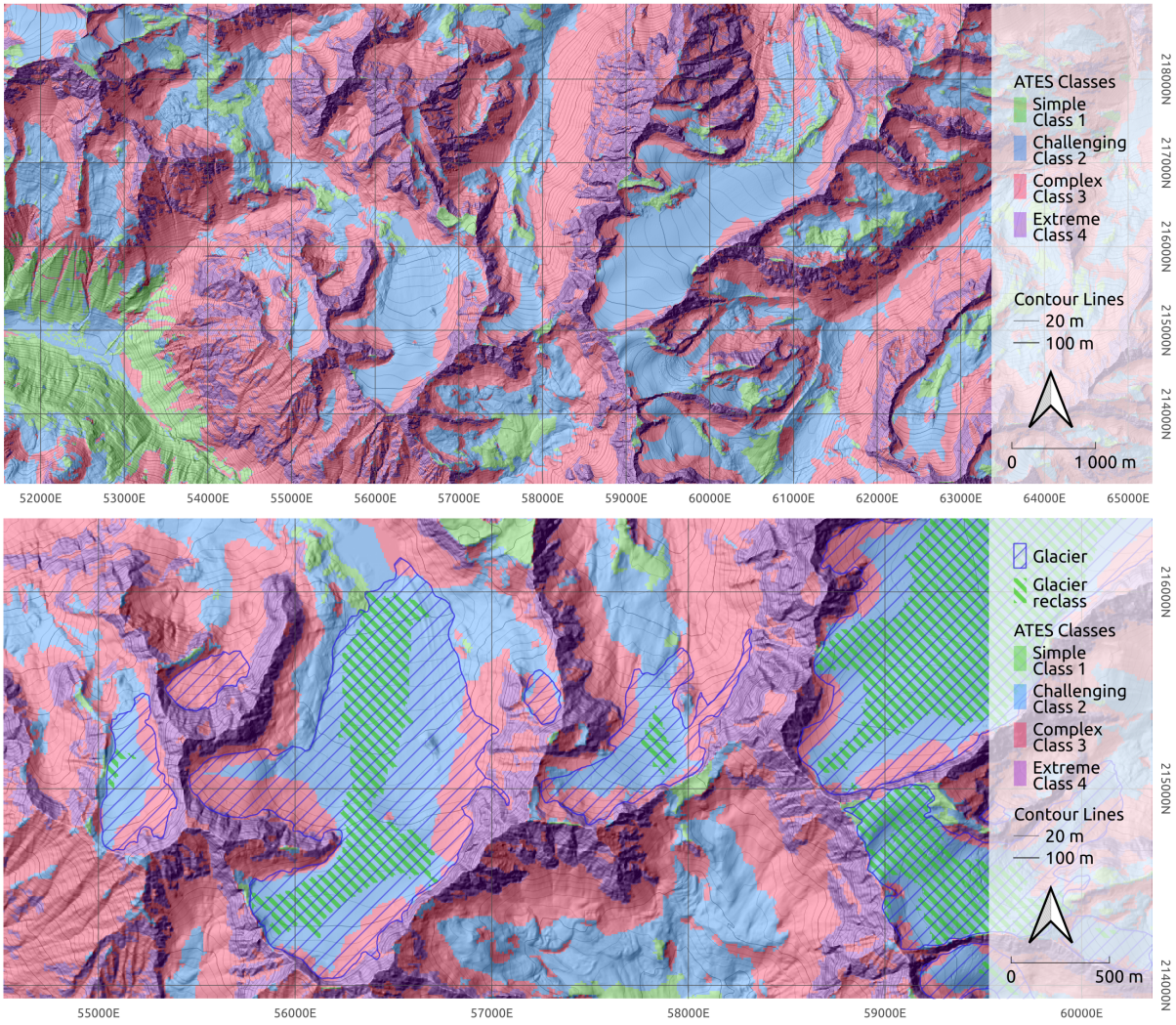


Figure 4: Final ATES map produced with the model parameters listed in table 3. The lower panel highlights the influence of glacier layer inclusion on the final map product (hashed green areas indicate glaciated areas, that have been reclassified from *simple* to *challenging*). The upper panel shows an overview of ATES classes for a larger portion of the study area popular with winter back-country users. Map-CRS is MGI/Austria GK West (EPSG: 31254), DEM from: data.tirol.gv.at issued under a CC-BY 4.0 license, glacier outlines from Buckel and Otto (2018) issued under a CC-BY 3.0 license.

## CODE AND DATA AVAILABILITY

The code for the AutoATES v2.0 model is available and maintained on github (`https://github.com/AutoATES/AutoATES-v2.0`, Toft et al. (2023b)). If you are interested in applying AutoATES in a new region using your own input data we recommend using this repository. In this study we used a slightly modified version of the AutoATES algorithm; if you are interested in reproducing the results of this study, please feel free to contact `andreas.huber@bfw.gv.at` for access to a separate code-repository containing the modified code and data used in this study.

## REFERENCES

Bauerhansl, C., Koukal, T., and Schadauer, C.: Erste österreichweite Waldkarte., Forstzeitung, 12, 26–27, 2007.

Buckel, J. and Otto, J.-C.: The Austrian Glacier Inventory GI 4 (2015) in ArcGis (shapefile) format, doi:10.1594/PANGAEA.887415, 2018.

Bühler, Y., Kumar, S., Veitinger, J., Christen, M., Stoffel, A., and Snehmani: Automated identification of potential snow avalanche release areas based on digital elevation models, Nat. Hazards Earth Syst. Sci., 13, 2013.

Bühler, Y., von Rickenbach, D., Stoffel, A., Margreth, S., Stoffel, L., and Christen, M.: Automated snow avalanche release area delineation – validation of existing algorithms and proposition of a new object-based approach for large-scale hazard indication mapping, Natural Hazards and Earth System Sciences, 18, 3235–3251, 2018.

Bühler, Y., Hafner, E., Zweifel, B., Zesiger, M., and Heisig, H.: Where are the avalanches? Rapid SPOT6 satellite data acquisition to map an extreme avalanche period over the Swiss Alps, The Cryosphere, 13, 3225 – 3228, 2019.

Bühler, Y., Bebi, P., Christen, M., Margreth, S., Stoffel, L., Stoffel, A., Marty, C., Schmucki, G., Caviezel, A., Kühne, R., Wohlwend, S., and Bartelt, P.: Automated avalanche hazard indication mapping on a statewide scale, Nat. Hazards Earth Syst. Sci., 22, 1825–1843, 2022.

Bühler, Y. and von Rickenbach, D.: Automated Avalanche Re-

lease Area (PRA) Delineation Davos, doi:http://dx.doi.org/10.16904/envidat.55, 2018.

CAA: OBSERVATION GUIDELINES AND RECORDING STANDARDS FOR WEATHER, SNOWPACK AND AVALANCHES, Tech. rep., Canadian Avalanche Association, 2016.

Campell, C. and Gould, B.: An ATES Zoning Model, The Avalanche Journal, 107, 26 – 29, 2014.

Campell, C. and Marshall, P.: Mapping Exposure to Avalanche Terrain, in: Proceedings, International Snow Science Workshop, Squaw Valley, USA, 2010, pp. 556 – 560, URL https://arc.lib.montana.edu/snow-science/item/442, 2010.

D'Amboise, C., Teich, M., Hormes, A., Steger, S., and Berger, F.: Protective forests as Ecosystem-based solution for Disaster Risk Reduction (ECO-DRR), chap. Modeling Protective Forests for Gravitational Natural Hazards and How It Relates to Risk-Based Decision Support Tools, IntechOpen, London, doi:10.5772/intechopen.99510, 2021.

D'Amboise, C. J. L., Neuhauser, M., Teich, M., Huber, A., Kofler, A., Perzl, F., Fromm, R., Kleemayr, K., and Fischer, J.-T.: Flow-Py v1.0: a customizable, open-source simulation tool to estimate runout and intensity of gravitational mass flows, Geosci. Model Dev., 15, 2423–2439, doi:https://doi.org/10.5194/gmd-15-2423-2022, 2022.

Delparte, D. M.: Avalanche Terrain Modeling in Glacier National Park, Canada, Phd thesis, University of Calgary, Calgary, Alberta, CAN, URL https://www.collectionscanada.gc.ca/obj/thesescanada/vol2/002/NR38205.PDF, 2008.

Harvey, S., Schmudlach, G., Bühler, Y., Dürr, L., Stoffel, A., and Christen, M.: Avalanche Terrain Maps for Backcountry Skiing in Switzerland, in: Proceedings, International Snow Science Workshop, Innsbruck, Austria, 2018, pp. 1625 – 1631, Innsbruck, Austria, 2018.

Heim, A.: Bergstürze und Menschenleben, in: Beiblatt zur Vierteljährsschrift der Naturforschenden Gesellschaft in Zürich, Fretz & Wasmuth, Zürich, CH, 1932.

Hesselbach, C.: Adaptaion and application of an automated Avalanche Terrain Classification in Austria, Masters' thesis, University of Life Sciences (BOKU), Vienna, Austria, 2023.

Horton, P., Jaboyedoff, M., Rudaz, B., and Zimmermann, M.: Flow-R, a model for susceptibility mapping of debris flows and other gravitational hazards at a regional scale, Nat. Hazards Earth Syst. Sci., 13, 869–885, doi:doi:10.5194/nhess-13-869-2013, 2013.

Körner, H.: The energy-line method in the mechanics of avalanches, Journal of Glaciology, 26, 501–505, 1980.

Landrø, M., Pfuhl, G., Engeset, R., Jackson, M., and Hetland, A.: Avalanche decision-making frameworks: Classification and description of underlying factors, Cold Regions Science and Technology, 169, 102 903, URL https://doi.org/10.1016/j.coldregions.2019.102903, 2020.

Larsen, H. T.: Using random forest to predict empircal avalanche runout, Masters' thesis, University of Oslo, Department of Geosciences, 2021.

Larsen, H. T., Hendrikx, J., Slåtten, M. S., and Engeset, R. V.: Developing nationwide avalanche terrain maps for Norway, Natural Hazards, 103, 2829 – 2847, doi:https://doi.org/10.1007/s11069-020-04104-7, 2020.

Maggioni, M. and Gruber, U.: The influence of topographic parameters on avalanche release dimension and frequency, Cold Region Science and Technology, 37, 407–419, doi:doi:10.1016/S0165-232X(03)00080-6, 2003.

Maggioni, M., Gruber, U., and Stoffel, A.: Definition and characterisation of potential avalanche release areas, in: ESRI International User Conference, pp. 1161–1166, San Diego, US, URL https://proceedings.esri.com/library/userconf/proc02/pap1161/p1161.htm, 2002.

Plattner, C., Braun, L. N., and Brenning, A.: Spatial variability of snow accumulation on Vernagtferner, Austrian Alps, in winter 2003/2004., Zeitschrift f"ur Gletscherkunde und Glazialgeologie, 39, 43–57, 2006.

Rauter, M., Paulus, G., and Seymann, C.: GIS-gestützte Analyse zur Berechnung potenzieller Lawinenabbruchgebiete, in: Angewandte Geoinformatik 2006, Beiträge zum 18. AGIT-Symposium, Salzburg, edited by Strobl, J., Blaschke, T., and Griesebner, G., pp. 569–578, Wichmann, Heidelberg, 2006.

Sappington, J. M., Longshore, K. M., and Thompson, D. B.: Quantifying Landscape Ruggedness for Animal Habitat Analysis: A Case Study Using Bighorn Sheep in the Mojave Desert, The Journal of Wildlife Management, 71, 1419–1426, URL https://www.jstor.org/stable/4496214, 2007.

Schmudlach, G. and Köhler, J.: Method for an automatized Avalanche Terrain Classification, in: Proceedings, International Snow Science Workshop, Breckenridge, Colorado, 2016, pp. 729 – 736, Breckenridge, Colorado, 2016.

Schumacher, J., Tøft, H., McLean, J. P., Hauglin, M., Astrup, R., and Breidenbach, J.: The utility of forest attribute maps for automated Avalanche Terrain Exposure Scale (ATES) modelling, Scandinavian Journal of Forest Research, 37, 264 – 275, 2022.

Schweizer, J., Jamieson, J. B., and Schneebli, M.: Snow Avalanche Formation, Reviews of Geophysics, 41, 2–1 – 2–25, URL https://doi.org/10.1029/2002RG000123, 2003.

Sharp, A. E. A.: Evaluating the exposure of heliskiing ski guides to avalanche terrain using a fuzzy logic avalanche susceptibility model, Masters' thesis, University of Leeds, School of Geography, 2018.

Statham, G.: Update to the Avalanche Terrain Exposure Scale, Presentation at CSAW 2020, https://www.oegsl.at/update-to-the-avalanche-terrain-exposure-scale/ (accessed: 23.08.2023), 2020.

Statham, G. and Campell, C.: The Avalanche Terrain Exposure Scale v2.0, Manuscript in preparation, 2023.

Statham, G., McMahon, B., and Tomm, I.: The Avalanche Terrain Exposure Scale, in: Proceedings of the 2006 International Snow Science Workshop, Telluride, Colorado, pp. 491 – 497, Telluride, Colorado, 2006.

Sykes, J., Haegeli, P., and Bühler, Y.: Automated snow avalanche release area delineation in data-sparse, remote, and forested regions, Natural Hazards and Earth System Sciences, 22, 3247 – 3270, URL https://doi.org/10.5194/nhess-22-3247-2022, 2022.

Tarboton, D. G.: TauDEM 5.3 GUIDE TO USING THE TAUDEM COMMAND LINE FUNCTIONS, online documentation https://hydrology.usu.edu/taudem/taudem5/TauDEM53CommandLineGuide.pdf (accessed: 23.08.2023), URL https://hydrology.usu.edu/taudem/taudem5/TauDEM53CommandLineGuide.pdf, 2016.

Toft, H. B., Müller, K., Hendrikx, J., Jaedicke, C., and Bühler, Y.: Can big data and random forests improve avalanche runout estimation compared to simple linear regression?, Cold Regions Science and Technology, 211, 103 844, URL https://doi.org/10.1016/j.coldregions.2023.103844, 2023a.

Toft, H. B., Sykes, J., and Schauer, A.: AutoATES v2.0, gitHub repository, URL https://github.com/AutoATES, https://github.com/AutoATES, 2023b.

Toft, H. B., Sykes, J., Schauer, A., Hendrikx, J., and Hetland, A.: AutoATES v2.0: Automated avalanche terrain exposure scale mapping., Manuscript in preparation, 2023c.

Tonnel, M., Wirbel, A., Oesterle, F., and Fischer, J.-T.: Avaframe com1DFA (version 1.3): a thickness integrated computational avalanche module - Theory, numerics and testing, EGUsphere [preprint], 2023.

Veitinger, J., Purves, R. S., and Sovilla, B.: Potential slab avalanche release area identification from estimated winter terrain: a multi-scale, fuzzy logic approach, Nat. Hazards Earth Syst. Sci., 16, 2211 – 2225, doi:doi:10.5194/nhess-16-2211-2016, 2016.

Wichmann, V.: The Gravitational Process Path (GPP) model (v1.0) – a GIS-based simulation framework for gravitational processes, Geosci. Model Dev.,, 10, 3309 – 3327, 2017.

Winstral, A., Elder, K., and Davis, R. E.: Spatial Snow Modeling of Wind-Redistributed Snow Using Terrain-Based Parameters, Journal of Hydrometeorology, 3, 524–538, 2002.